Rapid Communications

Quantum Monte Carlo calculations of weak transitions in $A = 6$–10 nuclei

S. Pastore,[1] A. Baroni,[2,3] J. Carlson,[1] S. Gandolfi,[1] Steven C. Pieper,[4] R. Schiavilla,[3,5] and R. B. Wiringa[4]

[1]*Theoretical Division, Los Alamos National Laboratory, Los Alamos, New Mexico 87545, USA*
[2]*Department of Physics and Astronomy University of South Carolina, Columbia, South Carolina 29208, USA*
[3]*Department of Physics, Old Dominion University, Norfolk, Virginia 23529, USA*
[4]*Physics Division, Argonne National Laboratory, Argonne, Illinois 60439, USA*
[5]*Theory Center, Jefferson Lab, Newport News, Virginia 23606, USA*

(Received 11 September 2017; revised manuscript received 30 November 2017; published 26 February 2018)

Ab initio calculations of the Gamow-Teller (GT) matrix elements in the β decays of ^{6}He and ^{10}C and electron captures in ^{7}Be are carried out using both variational and Green's function Monte Carlo wave functions obtained from the Argonne v_{18} two-nucleon and Illinois-7 three-nucleon interactions, and axial many-body currents derived from either meson-exchange phenomenology or chiral effective field theory. The agreement with experimental data is excellent for the electron captures in ^{7}Be, while theory overestimates the ^{6}He and ^{10}C data by $\sim$2% and $\sim$10%, respectively. We show that for these systems correlations in the nuclear wave functions are crucial to explaining the data, while many-body currents increase by $\sim$2–3% the one-body GT contributions.

DOI: 10.1103/PhysRevC.97.022501

A major objective of nuclear theory is to explain the structure and dynamics of nuclei in a fully microscopic approach. In such an approach the nucleons interact with each other in terms of many-body (primarily two- and three-body) effective interactions, and with external electroweak probes via effective currents describing the coupling of these probes to individual nucleons and many-body clusters of them. We will refer below to this approach as the *basic model* of nuclear theory.

For light nuclei (s- and p-shell nuclei up to ^{12}C), quantum Monte Carlo (QMC) and, in particular, Green's function Monte Carlo (GFMC) methods allow us to carry out accurate first-principles calculations of a variety of nuclear properties [1–3] within the basic model. These calculations retain the full complexity of the many-body correlations induced by the Hamiltonians and currents, which have an intricate spin-isospin operator structure. When coupled to the numerically accurate QMC methods, the deceptively simple picture put forward in the basic model provides a quantitative and accurate description of the structure and dynamics of light nuclei over a broad energy range, from the keV's relevant in nuclear astrophysical contexts [3–5], to the MeV's of low-lying nuclear spectra [3,6] and radiative decay processes [2,7], to the GeV's probing the short-range structure of nuclei and the limits of the basic model itself [2,8–10].

In the present study we focus on low-energy weak transitions in nuclei with mass number $A = 6$–10. In this mass range there are few microscopic calculations of Gamow-Teller (GT) matrix elements. Calculations based on the one-body GT operator have been performed, e.g., in Refs. [11,12]. To the best of our knowledge, calculations that account for many-body terms in addition to the one-body GT operator have been carried out in Refs. [13,14] (discussed below) and Refs. [15,16] which report on the ^{6}He β decay. However, most of the calculations of β decays and electron-capture processes in this mass range have mainly relied on relatively simple shell-model or cluster descriptions of the nuclear states involved in the transitions.

The shell model—itself an approximation of the basic model—has typically failed to reproduce the measured GT matrix elements governing these weak transitions, unless use is made of an effective one-body GT operator, in which the nucleon axial coupling constant g_A is quenched relative to its free value [17–19] (ranging from $g_A^{\rm eff} \simeq 0.85\, g_A$ in the light nuclei under consideration here to $g_A^{\rm eff} \simeq 0.7\, g_A$ in heavy nuclei). More phenomenological models have been based on α-nucleon-nucleon (for $A = 6$) or α-^{3}H and α-^{3}He (for $A = 7$) or α-α-nucleon-nucleon (for $A = 10$) clusterization, and have used Faddeev techniques with a separable representation of the nucleon-nucleon and α-nucleon interactions [20] or the resonating-group method [21] or rather crude potential wells [22]. While these studies provide useful insights into the structure of these light systems, nevertheless their connection to the basic model is rather tenuous. In particular, they do not explain whether the required quenching of g_A in shell-model calculations reflects deficiencies in the corresponding wave functions—possibly due to the lack of correlations and/or to limitations in model space—or in the model adopted for the nuclear axial current, in which many-body terms are typically neglected.

The first QMC calculation of the $A = 6$–7 weak transitions in the basic model was carried out with the variational Monte Carlo (VMC) method in Ref. [13]. It used nuclear axial currents including, apart from the (one-body) GT operator, two-body operators, which arise naturally in a meson-exchange picture (π- and ρ-exchange, and $\rho\pi$-transition mechanisms) and when excitations of nucleon resonances (notably the Δ isobar) are taken into account. These two-body operators, multiplied by hadronic form factors so as to regularize their short-range behavior in configuration space, were then constrained to reproduce the GT matrix element contributing to tritium β

decay by adjusting the poorly known N-to-Δ axial coupling constant (see Ref. [23] for a recent summary).

Yet, the calculations of Ref. [13] were based on *approximate* VMC wave functions to describe the nuclear states involved in the transitions. This shortcoming was remedied in the subsequent GFMC study of Ref. [14], which, however, only retained the one-body GT operator. Adding to the GFMC-calculated one-body matrix elements the VMC estimates of two-body contributions obtained in Ref. [13] led Pervin *et al.* [14] to speculate that a full GFMC calculation of these $A = 6$-7 weak transitions might be in agreement with the measured values.

The last three decades have witnessed the emergence of chiral effective field theory (χEFT) [24]. In χEFT, the symmetries of quantum chromodynamics (QCD), in particular its approximate chiral symmetry, are used to systematically constrain classes of Lagrangians describing, at low energies, the interactions of nucleons and Δ isobars with pions as well as the interactions of these hadrons with electroweak fields [25,26]. Thus χEFT provides a direct link between QCD and its symmetries, on one side, and the strong and electroweak interactions in nuclei, on the other. Germane to the subject of the present Rapid Comunication are, in particular, the recent χEFT derivations up to one loop of nuclear axial currents reported in Refs. [27,28]. Both these studies were based on time-ordered perturbation theory and a power-counting scheme *à la* Weinberg, but they adopted different prescriptions for isolating noniterative terms in reducible contributions.

There are differences in the loop corrections associated with box diagrams in these two independent derivations. It is plausible that a unitary transformation exists that allows one to go from the present representation of these corrections to that obtained by Krebs and collaborators [28]. Such a unitary equivalence relating loop corrections derived by our group [29] and the Bochum-Bonn group [30,31] was shown to hold in the case of the electromagnetic charge operator [29]. However, it has not yet been established whether this unitary equivalence remains valid for the axial currents under consideration here. Even so, as illustrated in the Supplemental Material [32] for the case of the GT matrix element in ^{3}H β decay, these differences are not expected to significantly affect the results reported below.

The present study reports on VMC and GFMC calculations of weak transitions in ^{6}He, ^{7}Be, and ^{10}C, based on the Argonne v_{18} (AV18) two-nucleon [33] and Illinois-7 (IL7) three-nucleon [34] interactions, and axial currents obtained either in the meson-exchange [23] or χEFT [27] frameworks mentioned earlier. The AV18+IL7 Hamiltonian reproduces well the observed spectra of light nuclei ($A = 3$–12), including the ^{12}C ground- and Hoyle-state energies [3]. The meson-exchange model for the nuclear axial current has been most recently reviewed in Ref. [23], where explicit expressions for the various one-body (1b) and two-body (2b) operators are also listed (including fitted values of the N-to-Δ axial coupling constant). The χEFT axial current [27,35] consists of 1b, 2b, and three-body (3b) operators. The 1b operators read

$$\mathbf{j}^{\rm 1b}_{5,\pm} = -g_A \sum_{i=1}^{A} \tau_{i,\pm} \left(\boldsymbol{\sigma}_i - \frac{\boldsymbol{\nabla}_i \, \boldsymbol{\sigma}_i \cdot \boldsymbol{\nabla}_i - \boldsymbol{\sigma}_i \, \nabla_i^2}{2\,m^2} \right), \quad (1)$$

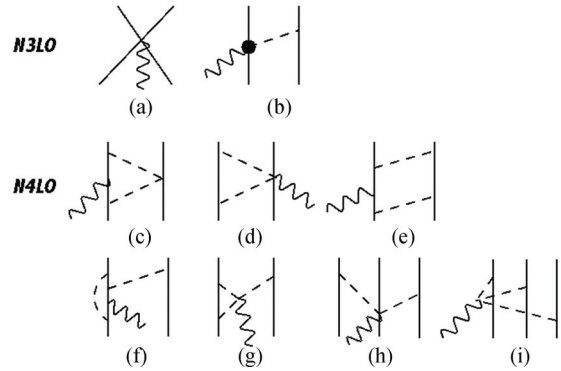

FIG. 1. Diagrams illustrating the (nonvanishing) contributions to the 2b and 3b axial currents. Nucleons, pions, and external fields are denoted by solid, dashed, and wavy lines, respectively. The circle in (b) represents the vertex implied by the $\mathcal{L}^{(2)}_{\pi N}$ chiral Lagrangian [36], involving the LECs c_3 and c_4. Only a single time ordering is shown; in particular, all direct- and crossed-box diagrams are accounted for. The power counting of the various contributions is also indicated. See text for further explanations.

where $\tau_{i,\pm} = (\tau_{i,x} \pm i\,\tau_{i,y})/2$ is the standard isospin raising (+) or lowering (−) operator, and $\boldsymbol{\sigma}_i$ and $-i\,\boldsymbol{\nabla}_i$ are, respectively, the Pauli spin matrix and momentum operator of nucleon i. The 2b and 3b operators are illustrated diagrammatically in Fig. 1 in the limit of vanishing momentum transfer considered here. Referring to Fig. 1, the 2b operators are from contact [CT, Fig. 1(a)], one-pion exchange (OPE) [Figs. 1(b) and 1(f)], and multipion exchange (MPE) [Figs. 1(c)–1(e) and 1(g)],

$$\mathbf{j}^{\rm 2b}_{5,\pm} = \sum_{i<j=1}^{A} \left[\mathbf{j}^{\rm CT}_{5,\pm}(ij) + \mathbf{j}^{\rm OPE}_{5,\pm}(ij) + \mathbf{j}^{\rm MPE}_{5,\pm}(ij) \right], \quad (2)$$

and the 3b operators are from MPE [Figs. 1(h)–1(i)],

$$\mathbf{j}^{\rm 3b}_{5,\pm} = \sum_{i<j<k=1}^{A} \mathbf{j}^{\rm MPE}_{5,\pm}(ijk)\,. \quad (3)$$

Configuration-space expressions for these 2b and 3b operators are reported in Ref. [35].

The 1b operator in Eq. (1) includes the leading-order (LO) GT term and the first nonvanishing corrections to it, which come in at next-to-next-to-leading order (N2LO) [35]. The latter are nominally suppressed by two powers of the expansion parameter Q/Λ_χ, where Q specifies generically the low-momentum scale and $\Lambda_\chi = 1$ GeV is the chiral-symmetry-breaking scale, but being inversely proportional to the nucleon mass m, itself of order Λ_χ, are in fact further suppressed than this naive power counting would indicate. Long-range 2b corrections from OPE enter at N3LO, Fig. 1(b), involving the low-energy constants (LECs) c_3 and c_4 in the subleading $\mathcal{L}^{(2)}_{\pi N}$ chiral Lagrangian [36], as well as at N4LO, Fig. 1(f). In terms of the expansion parameter Q/Λ_χ, they scale as $(Q/\Lambda_\chi)^3$ and $(Q/\Lambda_\chi)^4$, respectively, relative to the LO. Loop corrections from MPE, Figs. 1(c)–1(e) and 1(g), come in at N4LO, as do 3b currents, Figs. 1(h) and 1(i). Finally, the contact 2b current at N3LO, Fig. 1(a), is proportional to a LEC, denoted as z_0.

TABLE I. Gamow-Teller RMEs in $A = 6$, 7, and 10 nuclei obtained with chiral axial currents and GFMC (VMC) wave functions corresponding to the AV18+IL7 Hamiltonian model. Results corresponding to the one-body LO contribution (row labeled LO) and to the sum of all corrections beyond LO obtained with cutoff $\Lambda = 500$ and 600 MeV (rows labeled respectively as N4LO and N4LO*), are listed. The sum of all two-body corrections obtained with conventional meson-exchange axial currents is listed in the row labeled MEC. Cumulative contributions, to be compared with the experimental data [16,17,40,41] reported in the last row, are obtained by adding to the LO terms the contributions from either the chiral (N4LO or N4LO*) or the conventional (MEC) currents. Statistical errors associated with the Monte Carlo integrations are not shown, but are ∼1%.

	^{6}He β decay	^{7}Be ϵ capture (g.s.)	^{7}Be ϵ capture (ex)	^{10}C β decay
LO	2.168(2.174)	2.294(2.334)	2.083(2.150)	2.032(2.062)
N4LO	$3.73(3.03)\times10^{-2}$	$6.07(4.98)\times10^{-2}$	$4.63(4.63)\times10^{-2}$	$1.61(1.55)\times10^{-2}$
N4LO*	$3.62(3.43)\times10^{-2}$	$6.62(5.43)\times10^{-2}$	$5.31(5.38)\times10^{-2}$	$1.80(1.00)\times10^{-2}$
MEC	$6.90(4.57)\times10^{-2}$	$10.5(10.3)\times10^{-2}$	$8.88(8.99)\times10^{-2}$	$5.31(4.28)\times10^{-2}$
Expt.	2.1609(40)	2.3556(47)	2.1116(57)	1.8331(34)

The short-range behavior of the 2b and 3b operators is regularized by including a cutoff $C_\Lambda(k) = \exp(-k^4/\Lambda^4)$ in momentum space [35], and the values $\Lambda = 500$ and 600 MeV are considered in the present work. In correspondence to each Λ and to each set of (c_3, c_4), either $(c_3, c_4) = (-3.2, 5.4)$ GeV^{-1} as reported in Ref. [37] or $(c_3, c_4) = (-5.61, 4.26)$ GeV^{-1} as determined in Ref. [38], the LEC z_0 is constrained to reproduce the measured GT matrix element of tritium in hyperspherical-harmonics calculations based on the AV18+UIX [39] Hamiltonian [35]. While the three-nucleon potential employed in that work, the Urbana IX (UIX) model [39], is different from the IL7 adopted here, nevertheless both Hamiltonians, AV18+UIX and AV18+IL7, reproduce the empirical values for the trinucleon binding energies and charge radii. In particular, we find that the GFMC tritium GT matrix element obtained with the 1b axial current and AV18+IL7 Hamiltonian is within ∼3% of the experimental determination.

Reduced matrix elements (RMEs) for the β decays between the ^{6}He$(0^+;1)$ and ^{6}Li$(1^+;0)$ ground states, and between the ^{10}C$(0^+;1)$ ground state and ^{10}B$(1^+;0)$ first excited state, and ϵ captures of the ^{7}Be$(3/2^-;1/2)$ ground state to the ^{7}Li$(3/2^-;1/2)$ ground state and ^{7}Li$(1/2^-;1/2)$ first excited state are listed in Table I (in parentheses are the spin-parity J^π and isospin T assignments for each state). All processes are allowed or superallowed, and are therefore driven (almost) exclusively by the axial current (and, additionally, the vector charge—the Fermi operator—for the transition between the ground states of ^{7}Be and ^{7}Li). Retardation effects from the momentum transfer dependence of the operators, and corrections from suppressed transitions, such as, for example, those induced in the $A = 6$ and 10 decays by the magnetic dipole associated with the vector current, are negligible [13]. Therefore the RMEs listed in Table I follow simply from

$$\mathrm{RME} = \frac{\sqrt{2J_f+1}}{g_A}\,\frac{\langle J_f M|j^z_{5,\pm}|J_i M\rangle}{\langle J_i M, 10|J_f M\rangle}\,, \tag{4}$$

where $j^z_{5,\pm}$ is the z component of the axial current $\mathbf{j}_{5,\pm}$ (at vanishing momentum transfer) given above and $\langle J_i M, 10|J_f M\rangle$ are Clebsch-Gordan coefficients. The VMC results are obtained by straightforward Monte Carlo integration of the nuclear matrix elements above between (approximate) VMC wave functions; the GFMC results are from mixed-estimate evaluations of these matrix elements using previously generated GFMC configurations for the states under consideration, as illustrated in Ref. [14].

The sum of all contributions beyond LO, denoted as N4LO and N4LO* in Table I, leads approximately to a 2–3% increase in the LO prediction for the GT matrix elements of all processes under consideration. There is some cutoff dependence in these contributions, as indicated by the difference between the rows labeled N4LO and N4LO* in Table I, which may be aggravated here by the lack of consistency between the χEFT currents and the phenomenological potentials used to generate the wave functions, i.e., by the mismatch in the short-range behavior of potentials and currents. The N4LO and N4LO* results in Table I correspond to the set $(c_3, c_4) = (-3.2,\ 5.4)$ GeV^{-1} [37] in the OPE GT operator at N3LO. To illustrate the sensitivity of predictions to the set of (c_3, c_4) values, we observe that use of the more recent determination $(c_3, c_4) = (-5.61,\ 4.26)$ GeV^{-1} [38] would lead to an N4LO GFMC-calculated value of $6.71(2.89) \times 10^{-2}$ for the ^{7}Be ϵ capture to the ^{7}Li ground (first excited) state for the choice of cutoff $\Lambda = 500$ MeV, to be compared to the corresponding $6.07(4.63) \times 10^{-2}$ reported in Table I. Lastly, the N4LO contributions obtained with the more accurate GFMC wave functions are about 20% larger than those corresponding to VMC wave functions for the ^{6}He and ^{7}Be-to-^{7}Li ground-state transitions, albeit it should be emphasized that this is in relation a small overall ∼2% correction from 2b and 3b operators.

The contributions of the axial current order-by-order in the chiral expansion are given for the GT matrix element of the ^{7}Be ϵ capture in Table II. Those beyond LO, with the exception of the CT at N3LO, have opposite sign relative to the (dominant) LO. The loop corrections N4LO(2b) are more than a factor 5 larger (in magnitude) than the OPE. This is primarily due to the accidental cancellation between the terms proportional to c_3 and c_4 in the OPE operator at N3LO (which also occurs in the tritium GT matrix element [35]). It is also in line with the *chiral filter hypothesis* [42–46], according to which, if soft-pion processes are suppressed—as is the case for the axial current—then higher-order chiral corrections are not necessarily small. Indeed, the less than 3% overall correction due to terms beyond LO reported in Table I (row N4LO) comes about because of destructive interference between two relatively large (∼ 10%) contributions from the CT and the remaining [primarily N4LO(2b)] terms considered

TABLE II. Individual contributions to the ^{7}Be ϵ-capture Gamow-Teller RMEs obtained at various orders in the chiral expansion of the axial current ($\Lambda = 500$ MeV) with VMC wave functions. The rows labeled LO and N2LO refer to, respectively, the first term and the terms proportional to $1/m^2$ in Eq. (1); the rows labeled N3LO(CT) and OPE refer to Fig. 1(a) and Figs. 1(b) and 1(f), respectively; and N4LO(2b) and N4LO(3b) refer to Figs. 1(c)–1(e), 1(g) and Fig. 1(h), respectively.

	g.s.	ex
LO	2.334	2.150
N2LO	-3.18×10^{-2}	-2.79×10^{-2}
N3LO(CT)	2.79×10^{-1}	2.36×10^{-1}
OPE	-2.99×10^{-2}	-2.44×10^{-2}
N4LO(2b)	-1.61×10^{-1}	-1.33×10^{-1}
N4LO(3b)	-6.59×10^{-3}	-4.86×10^{-3}

here. Lastly, we note that going to N5LO (one order higher than in the present study) would introduce additional contact terms, thus reducing the predictive power of the theory, since the associated LECs would have to be determined by fitting, in addition to the ^{3}H β-decay rate, some of the weak rates discussed here.

Ratios of GFMC to experimental values for the GT RMEs in the ^{3}H, ^{6}He, ^{7}Be, and ^{10}C weak transitions are displayed in Fig. 2; theory results correspond to χEFT axial currents at LO and including corrections up to N4LO. The experimental values are those listed in Table I, while that for ^{3}H is 1.6474(24) [35]. These values have been obtained by using $g_A = 1.2723(23)$ [47] and $K/[G_V^2(1+\Delta_R^V)] = 6144.5(1.4)$ s [48], where $K = 2\pi^3 \ln 2/m_e^5 = 8120.2776(9) \times 10^{-10}$ GeV^{-4} s and $\Delta_R^V = 2.361(38)\%$ is the transition-independent radiative correction [48]. In the case of the β decays, but not for the ϵ captures, the transition-dependent (δ_R') radiative correction has also been accounted for. Lastly, in the ϵ processes the rates have been obtained by ignoring the factors B_K and B_{L1} which include the effects of electron exchange and overlap in the capture from the K and $L1$ atomic subshells. As noted by Chou *et al.* [17] following Bahcall [49,50], such an approximation

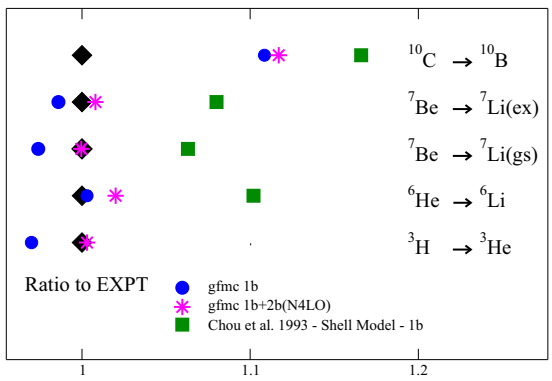

FIG. 2. Ratios of GFMC to experimental values of the GT RMEs in the ^{3}H, ^{6}He, ^{7}Be, and ^{10}C weak transitions. Theory predictions correspond to the χEFT axial current in LO (blue circles) and up to N4LO (magenta stars). Green squares indicate "unquenched" shell-model calculations from Ref. [17] based on the LO axial current.

is expected to be valid in light nuclei, since these factors only account for a redistribution of the total strength among the different subshells (however, it should be noted that B_K and B_{L1} were retained in Ref. [13], and led to the extraction of experimental values for the GT RMEs about 10% larger than reported here).

We find overall good agreement with data for the ^{6}He β decay and ϵ captures in ^{7}Be, although the former is over-predicted by $\sim 2\%$, a contribution that comes almost entirely from 2b and 3b chiral currents. The experimental GT RME for the ^{10}C β decay is overpredicted by $\sim$10%, with two-body currents giving a contribution that is comparable to the statistical GFMC error. The presence of a second $(1^+;0)$ excited state at $\sim$2.15 MeV can potentially contaminate the wave function of the ^{10}B excited state at $\sim$0.72 MeV, making this the hardest transition to calculate reliably. In fact, a small admixture of the second excited state ($\simeq$6% in probability) in the VMC wave function brings the VMC reduced matrix element in statistical agreement with the the measured value, a variation that does not spoil the overall good agreement we find for the reported branching ratios of 98.54(14)% (<0.08%) to the first (second) $(1^+,0)$ state of ^{10}B [17]. Because of the small energy difference of these two levels, it would require a computationally expensive GFMC calculation to see if this improvement remains or is removed; in lighter systems we have found that such changes of the trial VMC wave function are removed by GFMC.

We note that correlations in the wave functions significantly reduce the matrix elements, a fact that can be appreciated by comparing the LO GFMC (blue circles in Fig. 2) and the LO shell-model calculations (green squares in the same figure) from Ref. [17]. Moreover, preliminary variational Monte Carlo studies, based on the Norfolk two- and three-nucleon chiral potentials [6,51,52] and the LO GT operator, bring the ^{10}C prediction only $\sim$4% above the experimental datum [53], indicating that the $\sim$10% discrepancy we find here may indeed be attributable to deficiencies in the AV18+IL7 wave functions of $A = 10$ nuclei.

In the present study we have shown that weak transitions in $A = 6$–10 nuclei can be satisfactorily explained in the basic model without having to "quench" g_A. Clearly, in order to resolve the mismatch in the short-range behavior between potentials and currents alluded to earlier, GFMC calculations based on the Norfolk chiral potentials of Refs. [6,52] and consistent chiral currents are in order. Work along these lines is in progress.

ACKNOWLEDGMENTS

Correspondence with I.S. Towner in reference to radiative corrections in the $A = 6$–10 weak transitions is gratefully acknowledged. S.P. thanks A. Hayes for her guidance and numerous consultations on branching ratios in $A = 10$ decays. A.B. thanks H. Krebs and E. Epelbaum for correspondence in reference to the analytical comparison with the two-nucleon axial current operators derived in Ref. [28]. The work of S.P., J.C., S.G., S.C.P., and R.B.W. has been supported by the Nuclear Computational Low-Energy Initiative (NUCLEI) SciDAC project. The work of A.B. has been supported

by the U.S. Department of Energy, Office of Science, Office of Nuclear Physics, under Award No. DE-SC0010300. This research is also supported by the U.S. Department of Energy, Office of Science, Office of Nuclear Physics, under Contracts No. DE-AC05-06OR23177 (R.S.), No. DE-AC02-06CH11357 (S.C.P. and R.B.W.), and No. DE-AC52-06NA25396 and the Los Alamos LDRD program (J.C. and S.G.). Computational resources have been provided by Los Alamos Open Supercomputing, and Argonne's Laboratory Computing Resource Center. We also used resources provided by NERSC, which is supported by the U.S. DOE under Contract No. DE-AC02-05CH11231.

[1] J. Carlson and R. Schiavilla, Rev. Mod. Phys. **70**, 743 (1998), and references therein.
[2] S. Bacca and S. Pastore, J. Phys. G: Nucl. Part. Phys. **41**, 123002 (2014), and references therein.
[3] J. Carlson, S. Gandolfi, F. Pederiva, S. C. Pieper, R. Schiavilla, K. E. Schmidt, and R. B. Wiringa, Rev. Mod. Phys. **87**, 1067 (2015), and references therein.
[4] L. E. Marcucci, K. M. Nollett, R. Schiavilla, and R. B. Wiringa, Nucl. Phys. A **777**, 111 (2006), and references therein.
[5] E. G. Adelberger *et al.*, Rev. Mod. Phys. **83**, 195 (2011), and references therein.
[6] M. Piarulli, A. Baroni, L. Girlanda, A. Kievsky, A. Lovato, E. Lusk, L. E. Marcucci, S. C. Pieper, R. Schiavilla, M. Viviani, and R. B. Wiringa, Phys. Rev. Lett. **120**, 052503 (2018).
[7] S. Pastore, S. C. Pieper, R. Schiavilla, and R. B. Wiringa, Phys. Rev. C **87**, 035503 (2013).
[8] R. Schiavilla, R. B. Wiringa, S. C. Pieper, and J. Carlson, Phys. Rev. Lett. **98**, 132501 (2007).
[9] R. B. Wiringa, R. Schiavilla, S. C. Pieper, and J. Carlson, Phys. Rev. C **89**, 024305 (2014).
[10] L. E. Marcucci, F. Gross, M. T. Pena, M. Piarulli, R. Schiavilla, I. Sick, A. Stadler, J. W. Van Orden, and M. Viviani, J. Phys. G: Nucl. Part. Phys. **43**, 023002 (2016).
[11] P. Navratil and W. E. Ormand, Phys. Rev. C **68**, 034305 (2003).
[12] P. Navratil, V. G. Gueorguiev, J. P. Vary, W. E. Ormand, and A. Nogga, Phys. Rev. Lett. **99**, 042501 (2007).
[13] R. Schiavilla and R. B. Wiringa, Phys. Rev. C **65**, 054302 (2002).
[14] M. Pervin, S. C. Pieper, and R. B. Wiringa, Phys. Rev. C **76**, 064319 (2007).
[15] S. Vaintraub, N. Barnea, and D. Gazit, Phys. Rev. C **79**, 065501 (2009).
[16] A. Knecht, R. Hong, D. W. Zumwalt, B. G. Delbridge, A. Garcia, P. Muller, H. E. Swanson, I. S. Towner, S. Utsuno, W. Williams, and C. Wrede, Phys. Rev. C **86**, 035506 (2012).
[17] W.-T. Chou, E. K. Warburton, and B. A. Brown, Phys. Rev. C **47**, 163 (1993).
[18] J. Engel and J. Menendez, Rep. Prog. Phys. **80**, 046301 (2017); and references therein.
[19] A. Ekström *et al.*, Phys. Rev. Lett. **113**, 262504 (2014).
[20] W. C. Parke, A. Ghovanlou, C. T. Noguchi, M. Rajan, and D. R. Lehman, Phys. Lett. B **74**, 158 (1978).
[21] H. Walliser, Q. K. K. Liu, H. Kanada, and Y. C. Tang, Phys. Rev. C **28**, 57 (1983).
[22] F. J. Bartis, Phys. Rev. **132**, 1763 (1963).
[23] G. Shen, L. E. Marcucci, J. Carlson, S. Gandolfi, and R. Schiavilla, Phys. Rev. C **86**, 035503 (2012).
[24] S. Weinberg, Phys. Lett. B **251**, 288 (1990); Nucl. Phys. B **363**, 3 (1991); Phys. Lett. B **295**, 114 (1992).
[25] T.-S. Park, D.-P. Min, and M. Rho, Phys. Rep. **233**, 341 (1993); T.-S. Park, L. E. Marcucci, R. Schiavilla, M. Viviani, A. Kievsky, S. Rosati, K. Kubodera, D.-P. Min, and M. Rho, Phys. Rev. C **67**, 055206 (2003).
[26] T.-S. Park, D.-P. Min, and M. Rho, Nucl. Phys. A **596**, 515 (1996).
[27] A. Baroni, L. Girlanda, S. Pastore, R. Schiavilla, and M. Viviani, Phys. Rev. C **93**, 015501 (2016); **93**, 049902(E) (2016); **95**, 059901(E) (2017).
[28] H. Krebs, E. Epelbaum, and U.-G. Meissner, Ann. Phys. (NY) **378**, 317 (2017).
[29] S. Pastore, L. Girlanda, R. Schiavilla, and M. Viviani, Phys. Rev. C **84**, 024001 (2011).
[30] S. Kölling, E. Epelbaum, H. Krebs, and U.-G. Meissner, Phys. Rev. C **80**, 045502 (2009).
[31] S. Kölling, E. Epelbaum, H. Krebs, and U.-G. Meissner, Phys. Rev. C **84**, 054008 (2011).
[32] See Supplemental Material at http://link.aps.org/supplemental/10.1103/PhysRevC.97.022501 for calculations of the ^{3}Hβ decay matrix element based on loop corrections derived from Ref. [27] and Ref. [28].
[33] R. B. Wiringa, V. G. J. Stoks, and R. Schiavilla, Phys. Rev. C **51**, 38 (1995).
[34] S. C. Pieper, AIP Conf. Proc. **1011**, 143 (2008).
[35] A. Baroni, L. Girlanda, A. Kievsky, L. E. Marcucci, R. Schiavilla, and M. Viviani, Phys. Rev. C **94**, 024003 (2016); **95**, 059902(E) (2017).
[36] N. Fettes, U.-G. Meissner, M. Mojzis, and S. Steininger, Ann. Phys. (NY) **283**, 273 (2000); **288**, 249(E) (2001).
[37] R. Machleidt and D. R. Entem, Phys. Rep. **503**, 1 (2011).
[38] M. Hoferichter, J. Ruiz de Elvira, B. Kubis, and Ulf-G. Meissner, Phys. Rev. Lett. **115**, 192301 (2015).
[39] B. S. Pudliner, V. R. Pandharipande, J. Carlson, and R. B. Wiringa, Phys. Rev. Lett. **74**, 4396 (1995).
[40] W. Bambynek, H. Behrens, M. H. Chen, B. Crasemann, M. L. Fitzpatrick, K. W. D. Ledingham, H. Genz, M. Mutterer, and R. L. Intemann, Rev. Mod. Phys. **49**, 78 (1977).
[41] I. S. Towner (private communication).
[42] K. Kubodera, J. Delorme, and M. Rho, Phys. Rev. Lett. **40**, 755 (1978).
[43] M. Rho, Phys. Rev. Lett. **66**, 1275 (1991).
[44] M. Rho, *Chiral Nuclear Dynamics: From Quarks to Nuclei to Compact Stars* (World Scientific, Singapore, 2008).
[45] M. Rho, arXiv:1705.10864.
[46] Y.-L. Li, Y.-L. Ma, and M. Rho, arXiv:1710.02840.
[47] C. Patrignani *et al.* (Particle Data Group), Chin. Phys. C **40**, 100001 (2016).
[48] J. C. Hardy and I. S. Towner, Phys. Rev. C **91**, 025501 (2015).
[49] J. N. Bahcall, Phys. Rev. **129**, 2683 (1963).
[50] J. N. Bahcall, Rev. Mod. Phys. **50**, 881 (1978).
[51] M. Piarulli, L. Girlanda, R. Schiavilla, R. N. Perez, J. E. Amaro, and E. R. Arriola, Phys. Rev. C **91**, 024003 (2015).
[52] M. Piarulli, L. Girlanda, R. Schiavilla, A. Kievsky, A. Lovato, L. E. Marcucci, S. C. Pieper, M. Viviani, and R. B. Wiringa, Phys. Rev. C **94**, 054007 (2016).
[53] M. Piarulli (private communication).